Development of Nystagmus With the Absence of MYOD Expression in the Extraocular Muscles

Laura L. Johnson,[1,2] Rachel B. Kueppers,[1] Erin Y. Shen,[1] Jolene C. Rudell,[3] and Linda K. McLoon[1,2,4]

[1]Department of Ophthalmology and Visual Neurosciences, University of Minnesota Medical School, Minneapolis, Minnesota, United States
[2]Graduate Program in Molecular, Cellular, Developmental Biology and Genetics, University of Minnesota, Minneapolis, Minnesota, United States
[3]Department of Ophthalmology, University of California San Diego, San Diego, California, United States
[4]Stem Cell Institute, University of Minnesota Medical School, Minneapolis, Minnesota, United States

Correspondence: Linda K. McLoon, Department of Ophthalmology and Visual Neurosciences, University of Minnesota Medical School, Room 374, Lions Research Building, 2001 6th Street SE, Minneapolis, MN 55455, USA; mcloo001@umn.edu.

Received: March 3, 2021
Accepted: September 15, 2021
Published: October 7, 2021

Citation: Johnson LL, Kueppers RB, Shen EY, Rudell JC, McLoon LK. Development of nystagmus with the absence of MYOD expression in the extraocular muscles. *Invest Ophthalmol Vis Sci.* 2021;62(13):3. https://doi.org/10.1167/iovs.62.13.3

Purpose. Myoblast determination protein 1 (MYOD) is a critical myogenic regulatory factor in muscle development, differentiation, myofiber repair, and regeneration. As the extraocular muscles significantly remodel their myofibers throughout life compared with limb skeletal muscles, we hypothesized that the absence of MYOD would result in their abnormal structure and function. To assess structural and functional changes in the extraocular muscles in *MyoD*$^{-/-}$ mice, fiber size and number and optokinetic nystagmus reflex (OKN) responses were examined.

Methods. OKN was measured in *MyoD*$^{-/-}$ mice and littermate wild-type controls at 3, 6, and 12 months. The extraocular muscles were examined histologically for changes in mean myofiber cross-sectional area, total myofiber number, and nuclei immunostained for PAX7 and PITX2, markers of myogenic precursor cells.

Results. The *MyoD*$^{-/-}$ mice developed nystagmus, with both jerk and pendular waveforms, in the absence and in the presence of moving visual stimulation. At 12 months, there were significant losses in mean myofiber cross-sectional area and in total number of orbital layer fibers in all rectus muscles, as well as in global layer fibers in the superior and inferior rectus muscles. Haploinsufficient mice showed abnormal OKN responses. PITX2-positive cell entry into myofibers of the *MyoD*$^{-/-}$ mice was significantly reduced.

Conclusions. This study is the first demonstration of the development of nystagmus in the constitutive absence of expression of the muscle-specific transcription factor MYOD. We hypothesize that myofiber loss over time may alter anterograde and/or retrograde communication between the motor nerves and extraocular muscles that are critical for maintaining normalcy of extraocular muscle function.

Keywords: nystagmus, optokinetic nystagmus, extraocular muscles, morphometry

The extraocular muscles have a number of properties that make them structurally and functionally different from most other skeletal muscles. In contrast to most other skeletal muscles, the extraocular muscles undergo continuous myofiber remodeling throughout life.[1–5] The myogenic precursor cells within the extraocular muscle divide and fuse into existing myofibers, and this process results in significant myonuclear turnover throughout life, a process demonstrated by timed bromodeoxyuridine studies[1,4] and timed studies using a *Pax7*-reporter mouse.[5,6] This process depends on the two main myogenic precursor cell populations within the extraocular muscles: PAX7-positive cells, which are elevated in number compared to limb skeletal muscle,[7] and PITX2-positive cells, which are uniquely elevated in the extraocular muscles.[8]

Myoblast determination protein 1 (MYOD) is a transcription factor that plays an important role in myogenic cell determination and differentiation.[9,10] Both the PITX2 and PAX7 myogenic precursor cells activate MYOD, as MYOD is one of the first molecular steps toward myogenic differentiation. MYOD-positive cells are common during muscle development but gradually decrease in number in normal limb skeletal muscle unless injured or diseased.[11] However, MYOD-positive cells are easily identified in the adult extraocular muscles,[1–4] including human extraocular muscles from elderly individuals.[3] When *MyoD*$^{-/-}$ mice were developed, interestingly there was no overt muscle pathology in the limb skeletal muscles that were studied.[12] Further study showed that mice with a deletion of MYOD in limb skeletal muscles had a differentiation-defective phenotype in vitro,[13,14] as well as a regeneration deficient phenotype in vivo.[15,16] The effect of loss of MYOD expression has not been examined in the extraocular muscles. In light of the fact that the extraocular muscles have continuous and life-long myonuclear addition and turnover,[4,5] we hypothesized that loss of MYOD in skeletal muscle would result in abnormal

extraocular muscle structure and function compared with normal. One way to analyze extraocular muscle function and integrity is by measuring the optokinetic nystagmus (OKN) response, which works very effectively in humans, as well as in mice, to determine normal and abnormal eye movements.[17,18] We examined the OKN response in the *MyoD*$^{-/-}$ mice to assess if their eye muscles were functioning normally compared with wild-type littermate controls. Additionally, we determined myofiber cross-sectional areas and total myofiber number in the extraocular muscles from the *MyoD*$^{-/-}$ mice compared with their littermate controls at 3, 6, and 12 months of age to determine if the absence of MYOD expression would alter these characteristics in a muscle with such a high rate of myofiber remodeling.

As studies have shown that both myogenic precursor cell populations normally express MYOD before fusing into existing myofibers,[19] we hypothesized that, in the absence of MYOD, the ability to maintain myofiber size and number might be impacted, resulting in altered muscle function and nystagmus. To assess if the absence of MYOD expression affected muscle precursor cell populations in the extraocular muscles of the *MyoD*$^{+/+}$ and *MyoD*$^{-/-}$ mice, expression of two transcription factors was assessed. PAX7-positive nuclei were analyzed to identify quiescent satellite cells.[7] PITX2-positive nuclei, which identify a second population of muscle precursor cell with myogenic potential, were analyzed with respect to their position relative to dystrophin immunostaining, based on its localization to the cytoplasmic face of the sarcolemma.[8]

Methods

MyoD$^{+/-}$ mice were used to produce *MyoD*$^{+/+}$, *MyoD*$^{+/-}$, and *MyoD*$^{-/-}$ littermates.[12] The mice were housed and maintained by Research Animal Resources (St. Paul, MN, USA). All experiments were approved by the Institutional Animal Care and Use Committee at the University of Minnesota and adhered to the animal use recommendations of the National Institutes of Health and the Association for Research in Vision and Ophthalmology. Animals were maintained in a 12-hour light/dark cycle with food and water ad libitum.

OKN responses were measured using a custom-built device (ISCAN, Woburn, MA, USA). Mice received surgically implanted head posts to stabilize the head during testing. Head posts were implanted by first inserting 000 × 3/32″ self-tapping screws into the mouse skull on the top of the head. Geristore dental cement (DenMat Holdings LLC, Lompoc, CA, USA) was placed on top of the screws and surrounding skull area to create a cap in which to insert the head posts. M3 × 0.5 nylon pan head slotted screws, with the screw head removed, were placed vertically into the Geristore cement before it dried; this created posts on the mouse head for stabilization during experiments. When the mice had recovered from the head-post surgery, their eye movements were recorded by placing them in a dark room and immobilizing them with a clamp attached to the head posts and a tube around their bodies. During testing, the mice were surrounded by a white circular drum with black bars projected onto the white background. The black bars moved left to right across the mouse's vision field with varying spatial frequencies and varying contrasts, and eye movements tracking these rotating bars were recorded using a camera and the ISCAN program. The ISCAN program measures horizontal and vertical components of the movements of the mouse pupil, using a corneal reflection created by a red light near the camera aimed on the mouse eye. Calibration for each mouse was done prior to recording eye movements using both no stimuli and stimuli in the ISCAN program to set the detection of the whole pupil and the corneal reflection. To analyze the data from the ISCAN program, raw files of horizontal and vertical movement components were uploaded into a custom program in R (R Foundation for Statistical Computing, Vienna, Austria), where the raw pupil trace was filtered by subtracting the raw corneal reflection trace. The average vertical and horizontal positions were calculated for each trace. The graphs for each horizontal trace were centered at zero using this average, and the vertical trace was centered at –20 for ease of graphic representation. OKN responses were characterized based on published waveform analyses.[18]

MyoD$^{-/-}$ mice and *MyoD*$^{+/+}$ control littermates were euthanized, and the globes and attached extraocular muscles were removed as one tissue block. These were embedded in tragacanth gum oriented with the tendon end as the cutting edge and then frozen in 2-methylbutane chilled on liquid nitrogen. Blocks were sectioned at 10 µm. Representative sections, at 400 and 500 µm from the start of muscle in the cross-sections, were stained with hematoxylin and eosin to be used for morphometric analyses.

Mean cross-sectional areas and total fiber numbers were determined by manual tracing using the Bioquant Imaging Program (BIOQUANT Image Analysis Corporation, Nashville, TN, USA). A minimum of three sections were used to determine areas in each of the four rectus muscles from a minimum of five mice at each of the three ages: 3 months, 6 months, and 12 months. Means per muscle were determined for each mouse, and these means were used to determine the overall mean cross-sectional diameters of the individual rectus muscles.

PAX7-positive and PITX2-positive nuclei were assessed by morphometric analysis. Three sections per mouse from each *MyoD*$^{-/-}$ and *MyoD*$^{+/+}$ control littermates at each of the three ages were immunostained for the expression of PAX7 and PITX2 using our standard protocols.[4,8] Briefly, slides were quenched to remove endogenous peroxidase by incubation in 2% hydrogen peroxide in 0.01-M phosphate-buffered saline (PBS), rinsed in PBS, and fixed in ice-cold acetone for 10 minutes. After rinses in PBS, the sections were blocked with 10% horse serum in PBS containing 1% Triton X-100 (antibody buffer), followed by incubation with avidin/biotin blocking reagents to eliminate nonspecific binding (SP-2001; Vector Laboratories, Burlingame, CA, USA) using the vector kit instructions. After a PBS rinse, the slides were incubated for 1 hour with a PAX7 antibody (1:50 in antibody buffer; Hybridoma Bank PAX7c; University of Iowa, Iowa City, IA, USA) at room temperature in a humid chamber. The slides were rinsed in PBS and incubated with the secondary antibody using a VECTASTAIN Elite ABC system (HRP Kit, Peroxidase [Mouse IgG]; PK-6102; Vector Laboratories), followed by incubation in diaminobenzidine with heavy metal intensification. Sections were dehydrated, incubated in xylene, and coverslipped with Permount mounting medium (Thermo Fisher Scientific, Waltham, MA). For PITX2 immunostaining, sections were treated with blocking solution (20% goat serum, 0.2% bovine serum albumin in antibody buffer), followed by incubation in PITX2 antibody (1:150 in antibody buffer; PA-1020-100; Capra Science, Ängelholm, Sweden) for 1 hour at room temperature. After a PBS rinse, the sections were treated with blocking solution, followed by incubation in

Investigative Ophthalmology & Visual Science

Alexa Fluor 488 AffiniPure Goat Anti-Rabbit IgG (H+L) (1:1000; 111-545-144; Jackson ImmunoResearch Laboratories, West Grove, PA) for 30 minutes. The sections were rinsed and incubated with 10% rabbit serum, followed by overnight incubation at 4°C in AffiniPure Fab Fragment Goat Anti-Rabbit IgG (H+L) (1:100 in antibody buffer; 111-007-003; Jackson ImmunoResearch Laboratories). After a PBS rinse, the slides were treated with blocking solution for 10 minutes, followed by incubation for 1 hour at room temperature in antibody against dystrophin (1:150; ab15277; Abcam; Cambridge, UK). After a PBS rinse, the slides were again treated with blocking solution, followed by incubation for 30 minutes at room temperature with Rhodamine Red-X (RRX) AffiniPure Goat Anti-Rabbit IgG (H+L) (1:1000 in antibody buffer; 111-295-144; Jackson ImmunoResearch Laboratories). Dystrophin localizes to the cytoplasmic face of the sarcolemma and thus allows for distinction between myonuclei and nuclei that are outside the cell. After rinsing in PBS, the slides were coverslipped with VECTASHIELD Mounting Media (Vector Laboratories) and stored in the dark.

Analyses of these sections were performed on three slides from 3 animals each of the genotypes at each of the three ages by counting all positive nuclei in each microscopic field as a ratio of all myofibers in that field. If possible, a minimum of 200 myofibers were included in the analysis to ensure that representative numbers were obtained. The percent positive for each mouse was averaged for the three slides, and these averages were used to determine the percent positive nuclei per myofiber number for each genotype at each age. These analyses were performed for both transcription factors. All counting was performed in a masked manner. Data were analyzed using Prism (GraphPad Software, San Diego, CA, USA), with analysis of variance (ANOVA), and if a significant interaction was seen then post-hoc Tukey's multiple comparison tests were performed. Significance was defined as $P \leq 0.05$.

Results

Effects of Loss of MYOD Expression on Extraocular Muscle Function

Extraocular muscle function was tested using the OKN response. In normal mice, regardless of age, the OKN response was normal (Figs. 1A, 1B). In the absence of stimuli, the eyes were relatively unmoving in the normal mice. In the presence of the rotating black and white bars, a normal slow and fast phase characteristic of a normal OKN response was present. In the majority of *MyoD*$^{-/-}$ mice that were tested for OKN response, abnormal eye movements were present in the absence of visual stimuli (Figs. 1C, 1E, 1G, 1I). There was no connection between age of the mice and waveform abnormalities. These waveform abnormalities were present in all ages examined, even at the earliest age tested (3 months). In the absence of visual stimuli, 82% of the *MyoD*$^{-/-}$ mice examined had baseline jerk nystagmus mixed with asymmetric pendular movements, and generally they were characterized by erratic and irregular waveforms (Figs. 1G, 1I).[18] The other 18% of the *MyoD*$^{-/-}$ mice had pendular nystagmus in the absence of visual stimuli with occasional jerk-type movements (Figs. 1C, 1E). In the presence of the optokinetic stimuli, 50% of the *MyoD*$^{-/-}$ mice had pendular-like waveforms (Figs. 1D, 1F, 1H, 1J), even if they previously had a jerk-like waveform in the absence of stimuli (Figs. 1G–1J). There was no clear connection between pendular-type waveforms or jerk-type waveforms relative to age of the mice.

When mice that were haploinsufficient for *MyoD*$^{+/-}$ were tested, in the absence of optokinetic stimuli there were either occasional jerk movements or extended periods of jerk nystagmus (Figs. 2A, 2C). In the first example (Fig. 2A), in the absence of stimuli, there were only occasional jerk-like movements. In the presence of the OKN stimulus, the waveform was largely normal; however, there were flattened sections indicating extended foveation.[18] The second example shows that in the absence of stimuli oculomotor instability changes over time in an inconsistent pattern (Fig. 2C). In the presence of the OKN stimulus, although they again showed some normal tracking, they also showed intermittent interspersed jerk nystagmus-like movements (Figs. 2B, 2D).

Mean myofiber cross-sectional areas and total muscle fiber number were determined for each of the four rectus muscles compared with littermate control mice at 3, 6, and 12 months (Figs. 4, 5). At 3 months, the ANOVA indicated a significant interaction, but in the post hoc Tukey's multiple comparisons tests only the orbital layer fibers of the inferior rectus muscles were significantly smaller in mean cross-sectional area compared with controls ($P = 0.0355$) (Fig. 4A). At 6 months, although there were trends for decreased myofiber cross-sectional areas, the ANOVA did not show a significant interaction of the data between the *MyoD*$^{-/-}$ mice and controls (Fig. 4B). This is likely due to the increased variability over time in the absence of MYOD expression. For 12 months of age, the ANOVA showed a significant interaction based on genotype between the mean myofiber cross-sectional areas of the *MyoD*$^{-/-}$ mice and controls. The post hoc Tukey's multiple comparison tests demonstrated that the orbital layer myofibers of the superior and inferior rectus muscles were significantly smaller than the controls ($P = 0.0074$ and $P = 0.0009$, respectively), and similarly the global layer myofibers of the superior and inferior rectus muscles were significantly smaller than the controls ($P = 0.0064$ and $P = 0.0025$, respectively) (Figs. 3, 4C).

Total myofiber numbers were also calculated for the four rectus muscles in both the orbital and global layers of the *MyoD*$^{-/-}$ mice and compared to the littermate controls (Figs. 3, 5). In the 3-month-old *MyoD*$^{-/-}$ mice, the ANOVA showed there was a significant difference. However, post hoc *t*-tests showed that there were significantly fewer total numbers of myofibers only in the orbital medial rectus muscle ($P = 0.0001$) and in the global layers of the inferior and medial rectus muscles (inferior, $P = 0.0298$; medial, $P = 0.0015$) (Fig. 5A). Despite the downward trends for fiber number in all of the rectus muscles of the *MyoD*$^{-/-}$ mice at 6 months, none of the data was significantly different (Fig. 5B). By 12 months, however, ANOVA showed that the data were significantly different (Figs. 3, 5C). The post hoc *t*-tests showed that the orbital layers of all four rectus muscles from the *MyoD*$^{-/-}$ mice had significantly fewer myofibers than the littermate control mice (superior, $P = 0.0007$; inferior, $P = 0.0007$; medial, $P = 0.0007$; lateral, $P = 0.0242$) (Figs. 3, 5C). There were also significantly fewer global layer myofibers in the superior, inferior, and medial rectus muscles of the *MyoD*$^{-/-}$ mice compared with the littermate controls (superior, $P = 0.0022$; inferior, $P = 0.0065$; medial, $P = 0.046$) (Figs. 3, 5C).

Investigative Ophthalmology & Visual Science

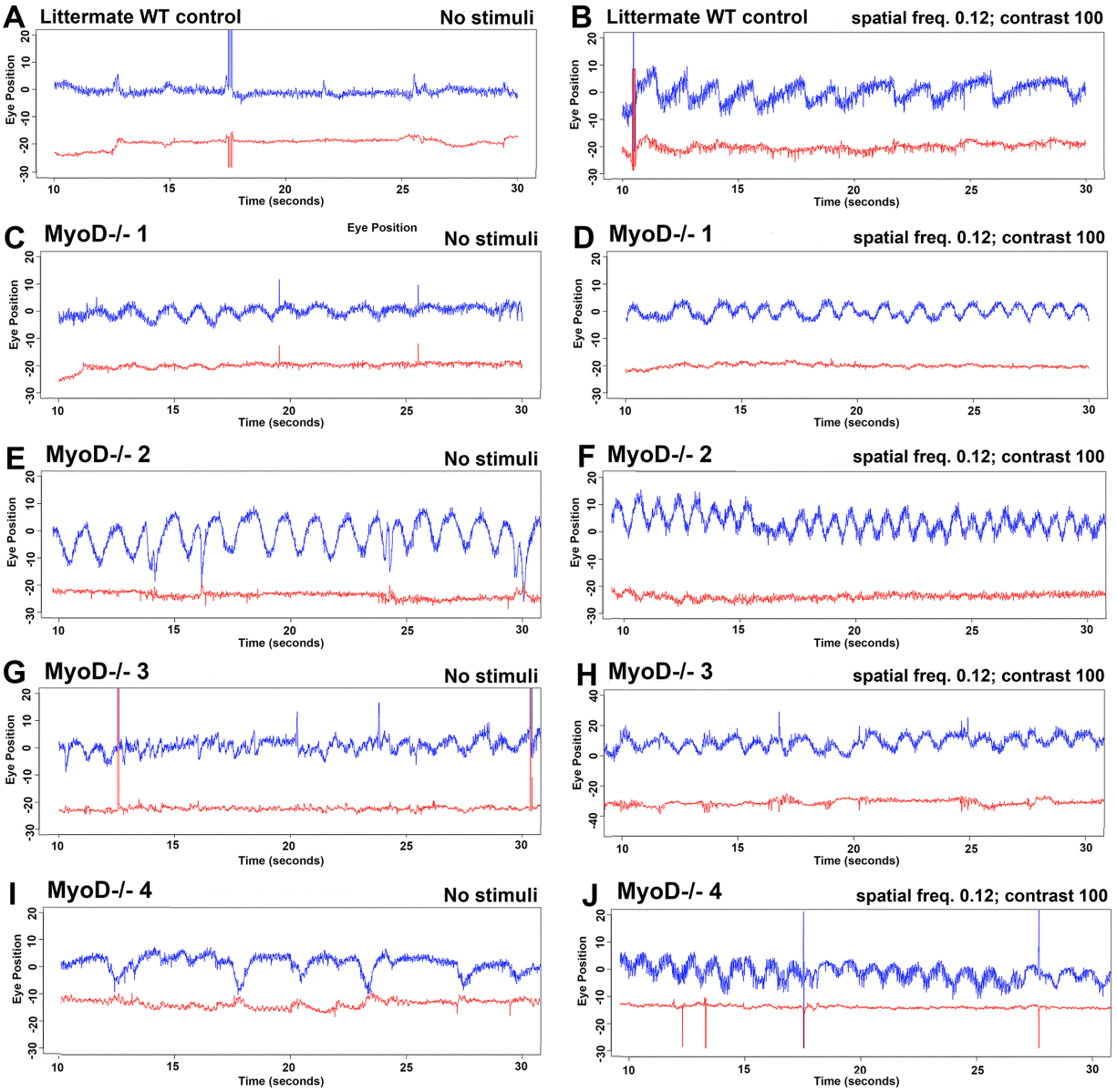

Figure 1. OKN responses for *MyoD*$^{-/-}$ compared with *MyoD*$^{+/+}$ (WT control) littermate controls. The graphs show eye position in horizontal (*blue line*) and vertical (*red line*) components as a function of time for 20 seconds. OKN was recorded using an ISCAN device. Eye movements were analyzed using a video camera to capture movements during no stimuli (**A**, **C**, **E**, **G**, **I**) and during stimuli of moving black bars on a white background with a spatial frequency of 0.12 and a contrast of 100 (**B**, **D**, **F**, **H**, **J**). *MyoD*$^{+/+}$ mice were used as a control and exhibited normal OKN (**A**, **B**) compared with *MyoD*$^{-/-}$ mice with differing waveforms of nystagmus (**C**–**J**). WT, wild-type.

PAX7-Positive Nuclear Analysis

The population of PAX7-positive nuclei based on myofiber number showed no significant differences in either the orbital or global layers at 3 and 6 months (Fig. 6). However, at 12 months, there was a significantly greater number of PAX7-positive cells, as percent of total myofiber number, in the global layer ($P = 0.0087$) of the *MyoD*$^{-/-}$ mice compared with their littermate WT controls, representing a 157.2% increase compared with controls.

PITX2-Positive Nuclear Analysis

PITX2-positive nuclei were identified as internal or external to dystrophin immunostaining, as the latter localizes to the cytoplasmic face of the sarcolemma (Fig. 7.) At 3 months, there was a significant alteration in location of the PITX2-positive nuclei, with a significant 63% decrease in the PITX2-positive myonuclei in the orbital layer of the extraocular muscles from the *MyoD*$^{-/-}$ mice ($P = 0.044$) and a significant 344.2% increase in the number of PITX2-positive nuclei outside the dystrophin immunostain ($P = 0.0006$) (Fig. 8). Similarly, there was a trend toward decreased myonuclei positive for PITX2 in the global layer of the extraocular muscles from the *MyoD*$^{-/-}$ mice (51% decrease). Analysis showed a significant 196.7% increase in the PITX2-positive nuclei outside the dystrophin immunostain in the *MyoD*$^{-/-}$ mice ($P = 0.048$). A similar picture was seen at 6 months, with a significant 80.4% decrease in the PITX2-positive myonuclei in the orbital layer of the extraocular

Investigative Ophthalmology & Visual Science

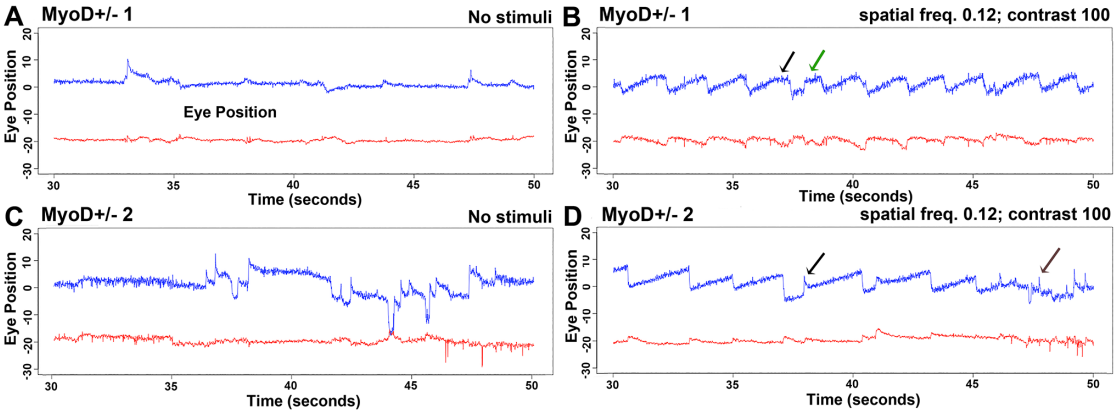

Figure 2. OKN responses for *MyoD*$^{+/-}$ mice. The graphs show eye position in horizontal (*blue line*) and vertical (*red line*) components as a function of time for 20 seconds. OKN was recorded using an ISCAN device. Eye movements were analyzed using a video camera to capture movements during no stimuli (**A**, **C**) and during stimuli of moving black bars on a white background with a spatial frequency of 0.12 and a contrast of 100 (**B**, **D**). In **A**, *green* and *black arrows* show flattened sections indicating extended foveation; in **B**, *black arrows* illustrate waveform variations within the normal OKN movements.

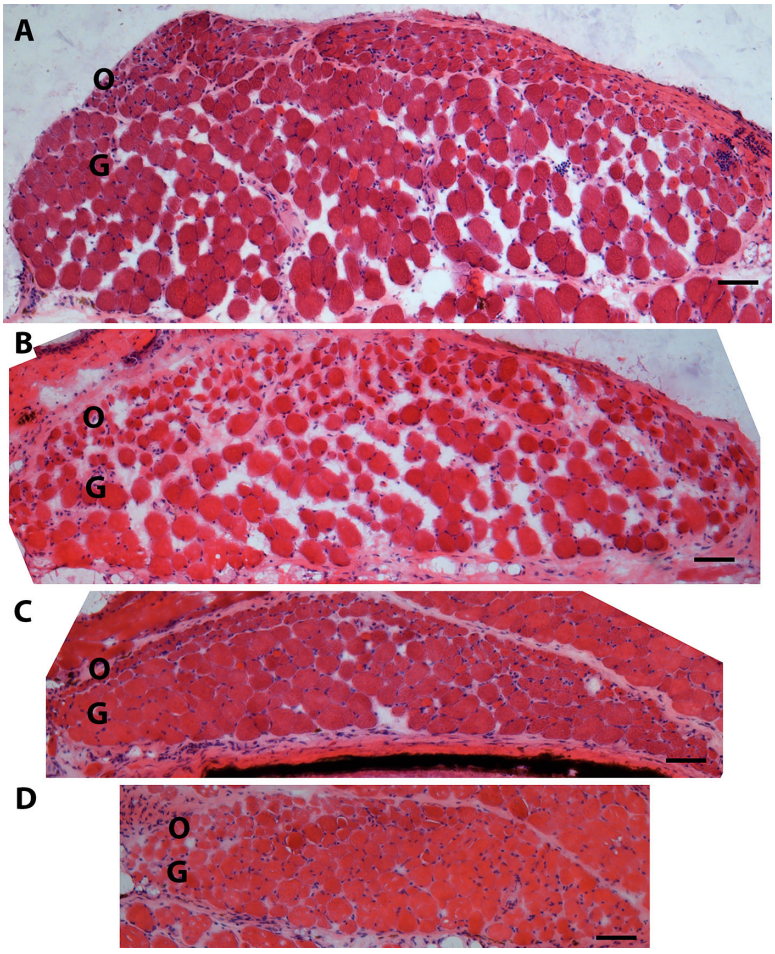

Figure 3. Photomicrographs of the superior rectus muscles of *MyoD*$^{+/+}$ and *MyoD*$^{-/-}$ mice at 12 months of age stained for hematoxylin and eosin. (**A**) Superior rectus muscle from a normal littermate *MyoD*$^{+/+}$ mouse. (**B**–**D**) Superior rectus muscles from *MyoD*$^{-/-}$ mice. Note that the orbital layer is thinner in these muscles than in the control, as well as the almost complete loss of the orbital layer in **D**. *Scale bar*: 50 µm. O, orbital layer; G, global layer.

Investigative Ophthalmology & Visual Science

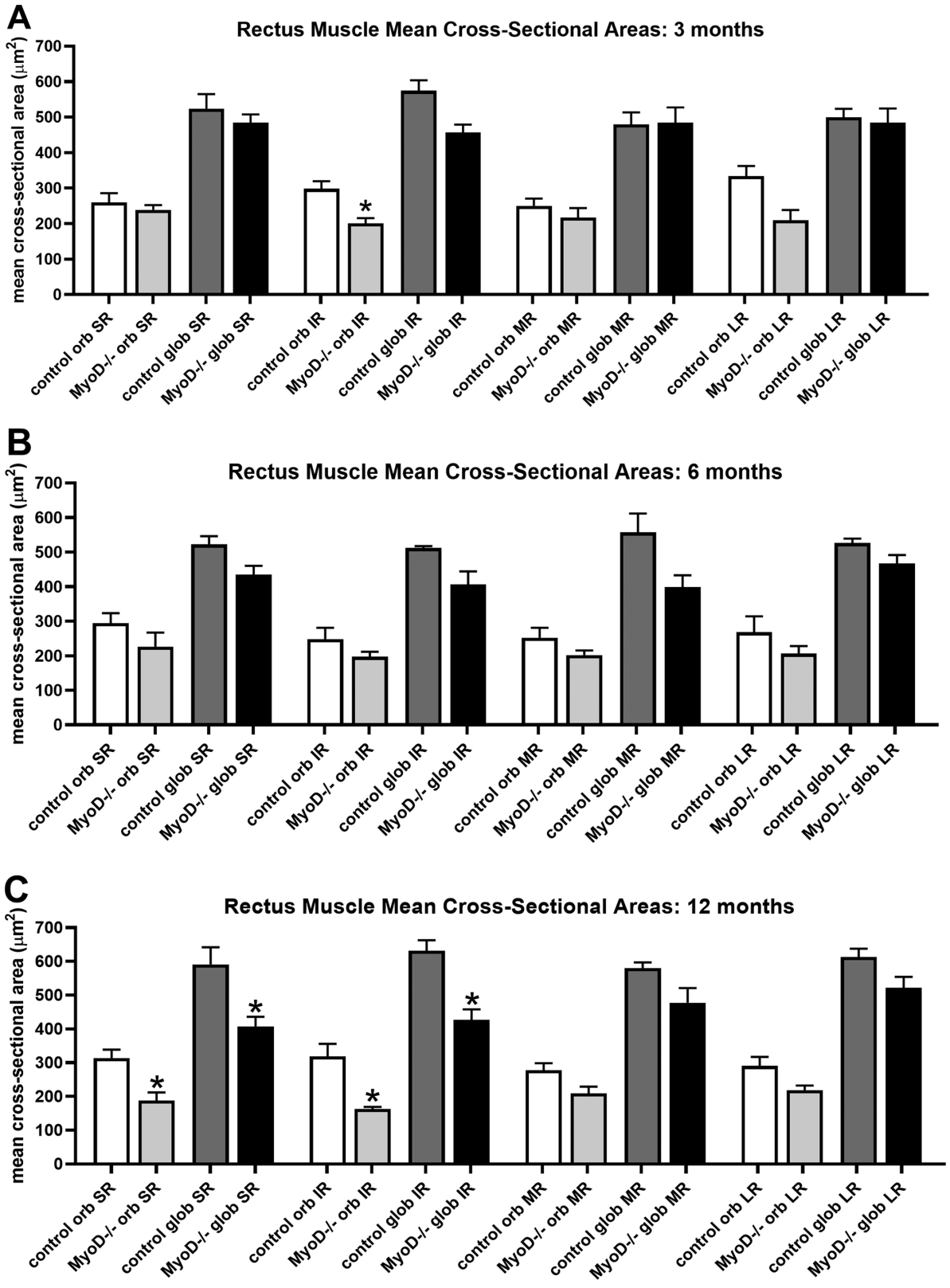

Figure 4. Mean myofiber cross-sectional areas of the superior rectus (SR), inferior rectus (IR), medial rectus (MR), and lateral rectus (LR) muscles from *MyoD*$^{+/+}$ (control) and *MyoD*$^{-/-}$ mice in both the orbital (orb) and global (glob) layers. Data represent animals at 3 months (**A**), 6 months (**B**), and 12 months (**C**). Asterisks indicate significant difference from the control fibers in the same layer of the muscles ($P < 0.05$).

Investigative Ophthalmology & Visual Science

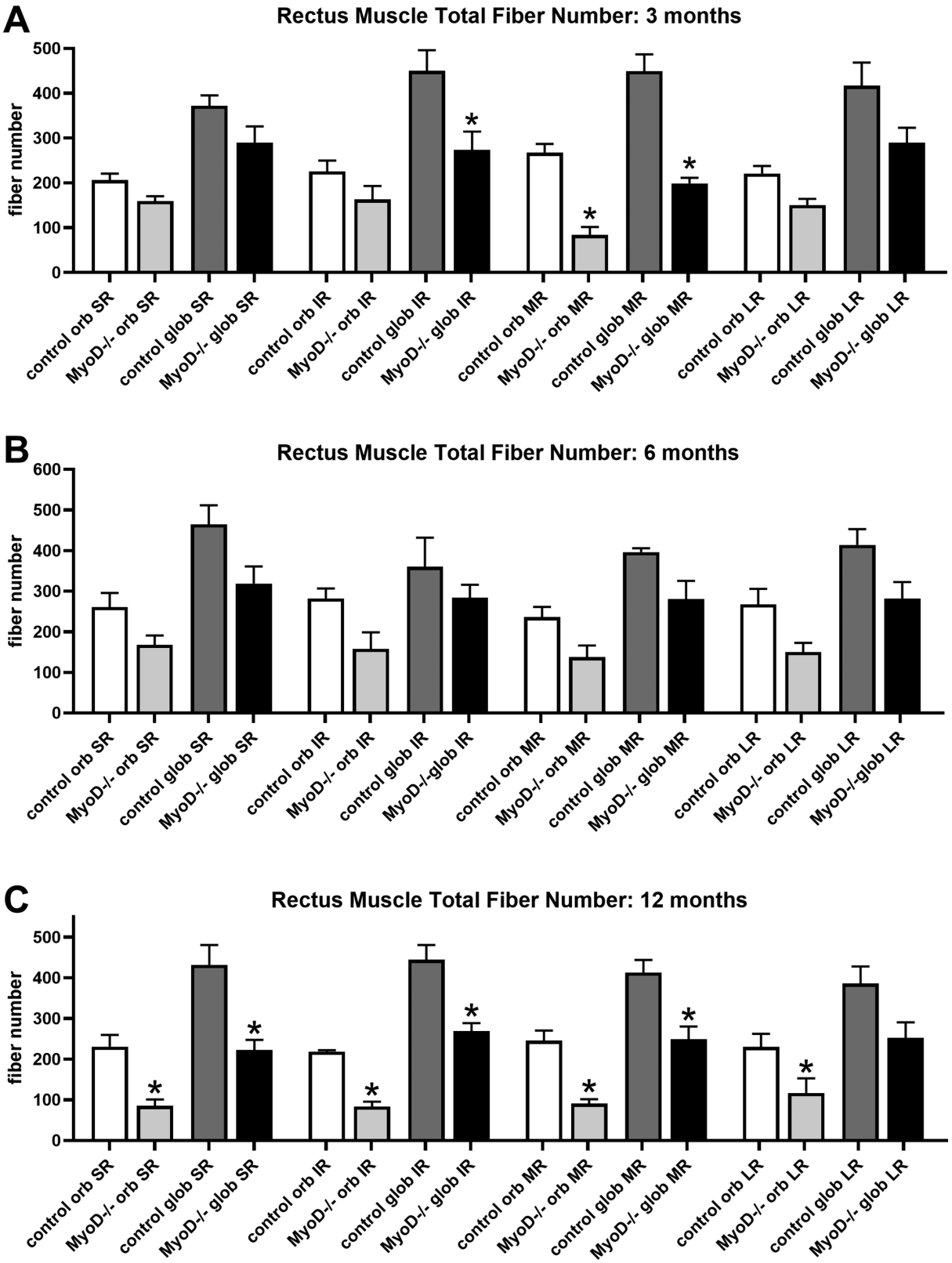

Figure 5. Mean total fiber numbers of the SR, IR, MR, and LR muscles from $MyoD^{+/+}$ (control) and $MyoD^{-/-}$ mice in both the orbital and global layers. Data represent animals at 3 months (**A**), 6 months (**B**), and 12 months (**C**). Asterisks indicate significant difference from the control fibers in the same layer of the muscles ($P < 0.05$).

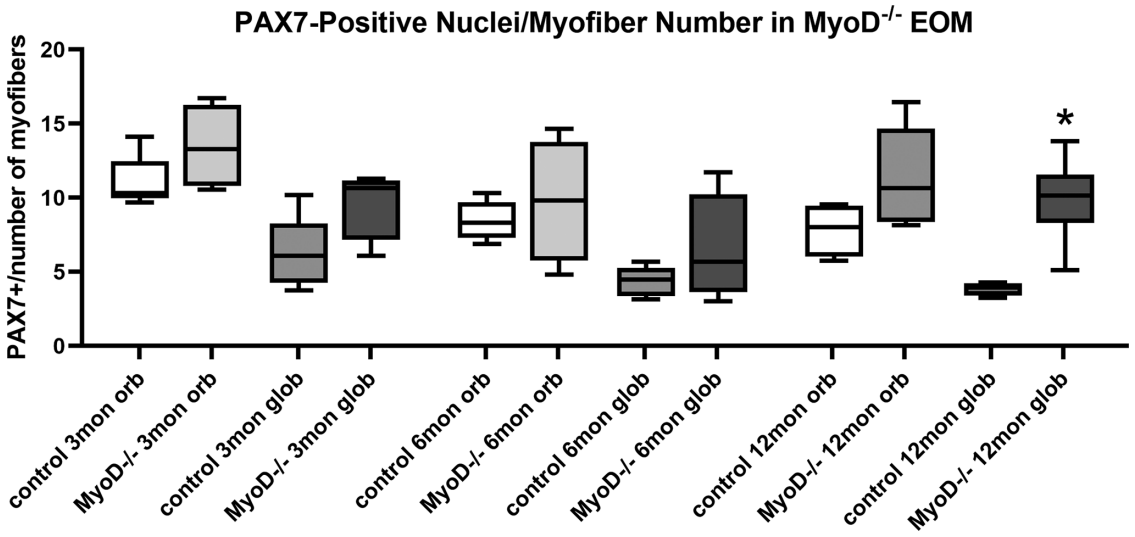

Figure 6. PAX7-positive nuclear numbers as a percent of total myofibers in extraocular muscles from *MyoD*$^{+/+}$ (control) and *MyoD*$^{-/-}$ mice. Asterisks indicate significant difference from the control fibers in the same layer of the muscles ($P < 0.05$). mon, month.

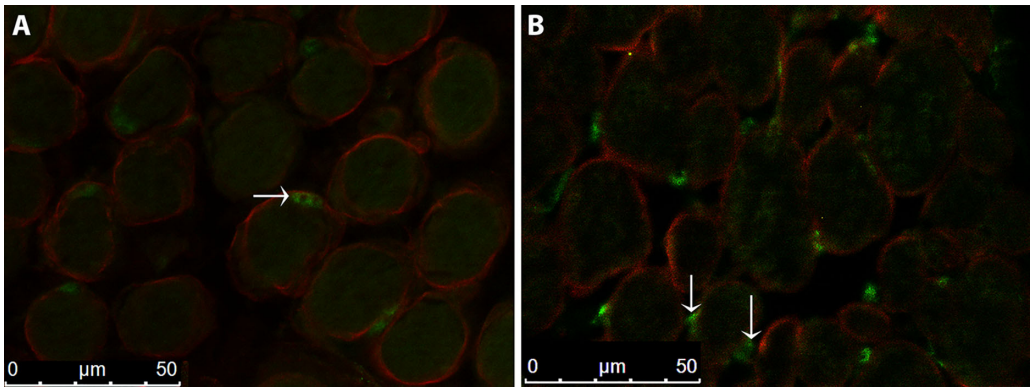

Figure 7. Photomicrograph of PITX2-positive nuclei in the extraocular muscles from (**A**) *MyoD*$^{+/+}$ (control) and (**B**) *MyoD*$^{-/-}$ mice at 6 months. *Horizontal arrow* indicates PITX2-positive myonucleus. *Vertical arrows* indicate PITX2-positive nuclei outside the dystrophin immunostaining.

muscles from the *MyoD*$^{-/-}$ mice ($P = 0.01$) (Figs. 7, 8) and a significant 346.9% increase in the number of PITX2-positive cells external to the dystrophin immunostain ($P = 0.046$). Similarly, there was a significant decrease in myonuclei positive for PITX2 in the global layer of the extraocular muscles from the *MyoD*$^{-/-}$ mice (79.7% decrease; $P = 0.01$) and a significant 205.7% increase in the PITX2-positive nuclei outside the dystrophin immunostain in the *MyoD*$^{-/-}$ mice ($P = 0.043$). At 12 months of age (Fig. 8), there was a significant 85.9% decrease in the PITX2-positive myonuclei in the orbital layer of the extraocular muscles from the *MyoD*$^{-/-}$ mice ($P = 0.0001$) (Fig. 8) and an 53.6% increase in the number of PITX2-positive cells outside the dystrophin immunostain, but this was not significant ($P = 0.066$). There was a significant decrease in myonuclei positive for PITX2 in the global layer of the extraocular muscles from the *MyoD*$^{-/-}$ mice (76.9% decrease; $P = 0.006$) and a significant 137.5% increase in the PITX2-positive nuclei outside the dystrophin immunostain in the *MyoD*$^{-/-}$ mice ($P = 0.049$).

Discussion

In the absence of expression of the transcription factor MYOD, all of the knockout mice developed some form of nystagmus. The presence of nystagmus correlated with significantly smaller myofiber cross-sectional areas and decreased total myofiber numbers in the *MyoD*$^{-/-}$ extraocular muscles over time. We hypothesize that, in the absence of normal myogenic precursor cell progression from quiescence to activation and myogenic differentiation during myofiber remodeling in the extraocular muscles in the *MyoD*$^{-/-}$ mice, the extraocular muscles would have a decreased ability to maintain their normal level of myofiber remodeling.[1,4] We also hypothesized that the sequelae to this would be a loss of either myofiber size or myofiber number. As previous studies showed a number of structural differences between the muscles of individuals with infantile nystagmus and age-matched controls,[20,21] we hypothesized that this would result in abnormal eye movements.

Investigative Ophthalmology & Visual Science

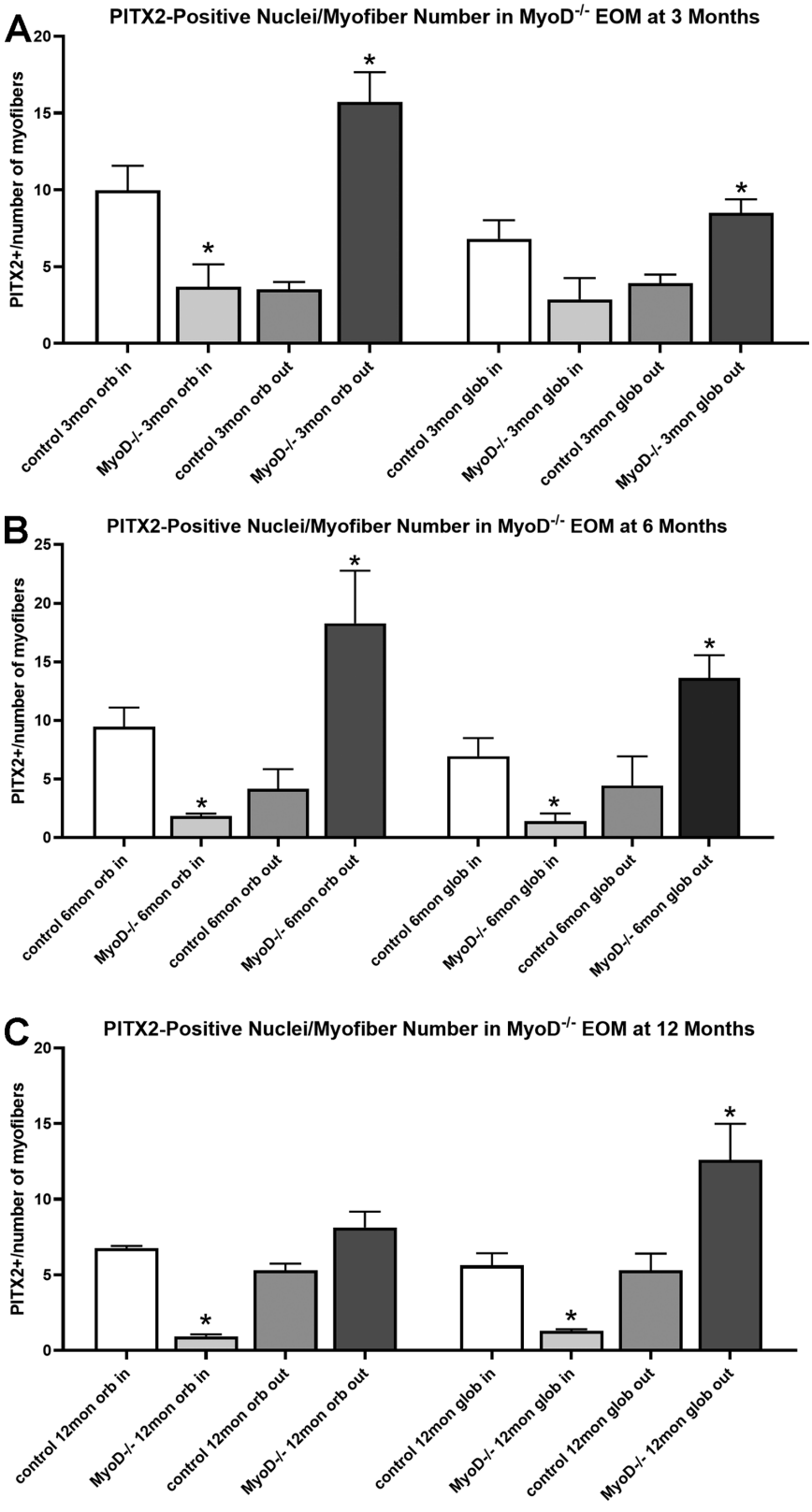

Figure 8. PITX2-positive nuclei as a percent of total fibers in extraocular muscles from *MyoD*$^{+/+}$ (control) and *MyoD*$^{-/-}$ mice at (**A**) 3 months, (**B**) 6 months, and (**C**) 12 months of age. "In" refers to PITX2-positive myonuclei, as defined by their location internal to the dystrophin immunostaining, and "out" refers to PITX2-positive nuclei outside the dystrophin immunostaining. Asterisks indicate significant difference from the control levels in the same layer of the muscles ($P < 0.05$).

Investigative Ophthalmology & Visual Science

Normally, MYOD functions to direct the commitment and ultimate differentiation of quiescent myogenic precursor cells into skeletal muscle during both development and regeneration.[22] In the absence of MYOD, limb skeletal muscle developed normally, with no clear morphological abnormalities.[12] Although other myogenic regulatory factors such as MYF5 are upregulated during embryonic development in the absence of MYOD expression,[12] in adult muscle MYOD plays a more critical role after muscle injury. Further study of the adult *MyoD*$^{-/-}$ mice showed them to be regeneration deficient, both in vitro[13,14] and in vivo.[15] Although no study examined the extraocular muscles in adult *MyoD*$^{-/-}$ mice prior to the current study, abnormal function was seen in the diaphragm muscles with decreased force generation and decreased contraction velocity.[23] Diaphragm also undergoes a significant level of myofiber remodeling compared to limb skeletal muscles, similar to that seen in the extraocular muscles.[5] This hypothesis is supported by the significant changes in the PITX2-positive population, which are thought to be critical for the significant level of myofiber remodeling seem in the extraocular muscles compared with limb skeletal muscles.[5,8] Our hypothesis is that the cells with the PITX2-positive nuclei, being unable to express MYOD and begin fusing into myofibers, accumulate on the outside of the sarcolemma. Similarly, by 12 months, the cells with PAX7-positive nuclei also begin to accumulate. We hypothesize that these changes are likely to have resulted in the decrease in both mean myofiber cross-sectional areas and total myofiber number as the animals aged.

Although there is no known association between *MyoD* mutations and eye movement disorders, it is interesting to note that recessive gene mutations of another myogenic regulatory factor, *myf5*, causes external ophthalmoplegia due to the complete absence of the extraocular muscles, along with an assortment of bony abnormalities.[24] Recently, MYOD was shown to be expressed in the cerebellum during development, where it played a role as a tumor suppressor gene in medulloblastoma.[25] When the cerebella of the *MyoD*$^{-/-}$ mice were examined, importantly no abnormalities were seen. Preliminary data from our laboratory examining the motor behavior of the *MyoD*$^{-/-}$ mice showed these mice to have normal levels of grip strength and normal levels of limb muscle coordination as examined using rotarod running of the *MyoD*$^{-/-}$ mice, even when they became quite old.

Classically, nystagmus is seen as a disturbance in central nervous system oculomotor pathways. Often, nystagmus is a clinical finding revealing an underlying central nervous system disease, and it may be the only manifestation of an insidious pathologic process in the brain.[26,27] Known genes associated with idiopathic infantile nystagmus independent of abnormal vision include the FERM domain-containing 7 gene (*FRMD7*). The FRMD7 protein is associated with neurite outgrowth and neuronal actin dynamics in growth cones, which suggests a role in axon guidance during neurodevelopment.[28,29]

In addition to central nervous system anomalies, a few studies have examined the extraocular muscles as a source of pathology in patients with infantile nystagmus. The extraocular muscles of patients with infantile nystagmus were found to have significantly decreased neuromuscular junctions and nerve fiber density in addition to abnormal extraocular muscle findings, including signs of increased myofiber turnover rate, although the myofiber cross-sectional areas were not different from non-nystagmus extraocular muscle controls.[20] A case study reported abnormal extraocular muscles in a patient with nystagmus, which was an incidental surgical finding during scleral buckle placement for retinal detachment repair.[30] The etiology of idiopathic congenital motor nystagmus is still unclear, although most studies focus on anomalies in the brain, with few studies implying there could be instances in these children of an abnormal change in the extraocular muscles and their innervation. The impact of the development of nystagmus caused by lack of MYOD expression on the developing visual system will be important for future studies to address.

It is interesting to note that the presence of nystagmus has been seen in individuals with congenital heart defects.[31,32] Because part of the heart muscle is derived from cranial head mesoderm,[33] it will be important for future genetic studies in children with infantile nystagmus syndrome to assess for genes related to head mesodermal development.

The results of this study demonstrate that nystagmus resulted from loss of expression of the protein MYOD due to a mutation in the *MyoD* gene. Even haploinsufficiency was sufficient to result in abnormalities in the OKN responses. Whether there is a correlate in human patients with idiopathic infantile nystagmus syndrome will require additional studies and genetic analyses, but these data support the possibility of such a mutation. As noted previously, mutations in *FRMD7* are associated with approximately 25% of cases of infantile nystagmus,[34] and specifically appear to regulate the length and branching of neurite outgrowth.[27] The hypothesized sequelae to this would include abnormal innervation of the extraocular muscles, which was shown by examination of surgical waste muscles from individuals having nystagmus surgery for improvement of head posture.[20,21] The muscle fibers from these children with infantile nystagmus had an increased presence of centrally nucleated myofibers, evidence of cycles of denervation/reinnervation, and decreased overall density of nerve fibers and neuromuscular junctions within the muscles compared with age-matched controls. Not only were the neuromuscular junctions smaller in the muscles in the surgical rectus muscle specimens, but there were also increased numbers of neuromuscular junctions with the immature gamma subunit on fast myofibers.[21] These previous studies support the view that the motor nerve–muscle feedback loops can be perturbed, and this perturbation correlates with the presence of nystagmus in both idiopathic infantile nystagmus and nystagmus associated with albinism. They also demonstrate that anterograde and/or retrograde communication between the motor nerves and the extraocular muscles are likely to be critical for maintaining normalcy of extraocular muscle function.

Acknowledgments

Supported by grants from the National Institutes of Health (R01 EY15313 to LKM; P30 EY11375) and the National Eye Institute, National Institutes of Health (T32 5T32AR007612-19 to LLJ) and by the Minnesota Lions Foundation.

Disclosure: **L.L. Johnson**, None; **R.B. Kueppers**, None; **E.Y. Shen**, None; **J.C. Rudell**, None; **L.K. McLoon**, None

References

1. McLoon LK, Wirtschafter JD. Continuous myonuclear addition to single extraocular myofibers in uninjured adult rabbits. *Muscle Nerve*. 2002;25:348–358.

2. McLoon LK, Wirtschafter JD. Activated satellite cells are present in uninjured extraocular muscles of mature mice. *Trans Am Ophthalmol Soc*. 2002;100:119–124.
3. McLoon LK, Wirtschafter JD. Activated satellite cells in extraocular muscles of normal adult monkeys and humans. *Invest Ophthalmol Vis Sci*. 2003;44:1927–1932.
4. McLoon LK, Rowe J, Wirtschafter J, McCormick KM. Continuous myofiber remodeling in uninjured extraocular myofibers: myonuclear turnover and evidence for apoptosis. *Muscle Nerve*. 2004;29:707–715.
5. Pawlikowski B, Pulliam C, Betta ND, Kardon G, Olwin BB. Pervasive satellite cell contribution to uninjured adult muscle fibers. *Skelet Muscle*. 2015;5:42.
6. Keefe AC, Lawson JA, Flygare SD, et al. Muscle stem cells contribute to myofibers in sedentary adult mouse. *Nat Commun*. 2015;6:7087.
7. Verma M, Fitzpatrick K, McLoon LK. Extraocular muscle repair and regeneration. *Curr Ophthalmol Rep*. 2017;5(3):207–215.
8. Hebert SL, Daniel ML, McLoon LK. The role of Pitx2 in maintaining the phenotype of myogenic precursor cells in the extraocular muscles. *PLoS One*. 2013;8:e58405.
9. Weintraub H, Davis R, Tapscott S, et al. The *MyoD* gene family: nodal point during specification of the muscle cell lineages. *Science*. 1991;251:761–766.
10. Grounds MD, Garrett KL, Lai MC, Wright WE, Beilharz MW. Identification of skeletal muscle precursor cells in vivo by use of MyoD1 and myogenin probes. *Cell Tissue Res*. 1992;267:99–104.
11. Koishi K, Zhang M, McLennan IS, Harris AJ. MyoD protein accumulates in satellite cells and is neutrally regulated in regenerating myotubes and skeletal muscle fibers. *Dev Dyn*. 1995;202:244–254.
12. Rudnicki MA, Braun T, Hinuma S, Jaenisch R. Inactivation of *MyoD* in mice leads to up-regulation of the myogenic HLH gene *Myf-5* and results in apparently normal muscle development. *Cell*. 1992;71:383–390.
13. Sabourin LA, Girgis-Gabrado A, Seale P, Asakura A, Rudnicki MA. Reduced differentiation potential of primary *MyoD*$^{-/-}$ myogenic cells derived from adult skeletal muscle. *J Cell Biol*. 1999;144:631–643.
14. Cornelison DDW, Olwin BB, Rudnicki RA, Wold BJ. MyoD$^{-/-}$ satellite cells in single fiber culture are differentiation defective and MRF4 deficient. *Dev Biol*. 2000;224:122–137.
15. White JD, Scaffidi A, Davies M, et al. Myotube formation is delayed but not prevented in MyoD-deficient skeletal muscle: studies in regenerating whole muscle grafts of adult mice. *J Histochem Cytochem*. 2000;48:1531–1543.
16. Yamamoto M, Legendre NP, Biswas AA, et al. Loss of *MyoD* and *Myf5* in skeletal muscle stem cells results in altered myogenic programming and failed regeneration. *Stem Cell Rep*. 2018;10:956–969.
17. Traber GL, Chen CC, Huang YY, et al. Albino mice as an animal for infantile nystagmus syndrome. *Invest Ophthalmol Vis Sci*. 2012;53:5737–5747.
18. Dell'Osso LF, Daroff RB. Congenital nystagmus waveforms and foveation strategy. *Doc Ophthalmol*. 1975;39:155–192.
19. Zammit PS, Relaix F, Nagata YH, et al. Pax7 and myogenic progression in skeletal muscle satellite cells. *J Cell Sci*. 2006;119:1824–1832.
20. Berg KT, Hunter DG, Bothun ED, Antunes-Foschini R, McLoon LK. Extraocular muscles in patients with infantile nystagmus. *Arch Ophthalmol*. 2012;130:343–349.
21. McLoon LK, Willoughby CL, Anderson JS, et al. Abnormally small neuromuscular junctions in the extraocular muscles from subjects with idiopathic nystagmus and nystagmus associated with albinism. *Invest Ophthalmol Vis Sci*. 2016;57:1912–1920.
22. Zammit PS. Function of myogenic regulatory factors Myf5, MyoD, myogenin, and MRF4 in skeletal muscle, satellite cells, and regenerative myogenesis. *Semin Cell Dev Biol*. 2017;72:19–32.
23. Staib JL, Swoap SJ, Powers SK. Diaphragm contractile dysfunction in MyoD gene-inactivated mice. *Am J Physiol Regul Integr Comp Physiol*. 2002;283:R583–R590.
24. Di Gioia SA, Shaaban S, Tüysüz B, et al. Recessive *MYF5* mutations cause external ophthalmoplegia, rib, and vertebral anomalies. *Am J Hum Genet*. 2018;103:115–124.
25. Dey J, Dubuc AM, Pedro KD, et al., MyoD is a tumor suppressor gene in medulloblastoma. *Cancer Res*. 2013;73:6828–6837.
26. Bertsch M, Floyd M, Kehoe T, Pfeifer W, Drack AV. The clinical evaluation of infantile nystagmus: what to do first and why? *Ophthalmic Genet*. 2017;38:22–33.
27. Peragallo JH. Effects of brain tumors on vision in children. *Int Ophthalmol Clin*. 2018;58:83–95.
28. Betts-Henderson J, Bartesaghi S, Crosier M, et al. The nystagmus-associated FRMD7 gene regulates neuronal outgrowth and development. *Hum Mol Genet*. 2010;19:342–351.
29. Watkins RJ, Thomas MG, Talbot CJ, Gottlob I, Shackleton S. The role of FRMD7 in idiopathic infantile nystagmus. *J Ophthalmol*. 2012;2012:460956.
30. Chaum E, Hatton MP. Congenital nystagmus associated with multiple congenital anomalies of the extraocular muscles. *J Pediatr Ophthalmol Strabismus*. 1999;36:155–157.
31. Bromham NR, Woodhouse JM, Cregg M, Webb E, Frazer WI. Heart defects and ocular anomalies in children with Down's syndrome. *Br J Ophthalmol*. 2002;86:1367–1468.
32. Ljubic A, Trajkovski V, Tesic M, Tojtovska B, Stankovic B. Ophthalmic manifestations in children and young adults with Down syndrome and congenital heart defects. *Ophthalmic Epidemiol*. 2015;22:123–129.
33. Tirosh-Finkel L, Elhanany H, Rinon A, Tzahor E. Meosderm progenitor cells of common origin contribute to the head musculature and the cardiac outflow tract. *Development*. 2006;133:1943–1953.
34. Tarpey P, Thomas S, Sarvananthan N, et al. Mutations in FRMD7, a newly identified member of the FERM family, cause X-linked idiopathic congenital nystagmus. *Nat Genet*. 2006;38:1242–1244.

Investigative Ophthalmology & Visual Science